Preliminary Spectroradiometric Measurements of the Solar Constant [1]

Ralph Stair and Russell G. Johnston

Spectroradiometric measurements of the distribution of direct solar radiation at Sunspot, New Mexico (altitude 9,200 feet), in June 1955 are described. Detailed spectral data were obtained within the spectral range of 299 to 535 millimicrons for different air masses. At longer wavelengths radiant-energy evaluations were made only for selected points between the water-absorption bands.

From these data, supplemented by other measurements and estimates for radiant-energy intensities for very short and very long wavelengths, a preliminary spectral integration of the total solar intensity yields a solar constant in general agreement with the best published values.

1. Introduction

Recent scientific advances in many fields have reached the stage where a higher accuracy in the knowledge of the intensity of the radiant energy from the sun is required. The present research has been carried out with the idea of obtaining a value of the solar constant by a method that is different from previous determinations.

During the past 30 years the Astrophysical Observatory of the Smithsonian Institution has accumulated a tremendous amount of spectral solar radiant energy data at a number of stations scattered over the world. These measurements have recently been supplemented by rocket data, which have extended the spectrum essentially to the ultraviolet cutoff of solar emission [1,2].[2]

The Smithsonian data are obtained by a method that requires a number of corrections. There is some question as to the precise value of some of these corrections [3,4,5,6,7]. Many of them result from the particular method employed in obtaining and evaluating the data [8].

In the Smithsonian work [9] the solar beam was reflected into a spectroradiometer by a metal-coated mirror whose reflectivity was subject to change with age. In measurements by this method the optical characteristics of the spectroradiometer would need to be evaluated for light reflected from various angles. It is difficult to obtain this correction with a high precision. Because an image of the solar disk was focused upon the entrance slit of the spectrometer, any attempt to evaluate the data in terms of an average value for the complete disk would be subject to doubt.

In addition, an attempt to integrate the data for the complete spectrum in absolute value was made by employing a pyrheliometer in the measurement of the total radiant energy coming through the atmosphere. This involved a number of corrections because of water vapor and other absorptions in the atmosphere, as well as assumptions regarding the spectral limits of the two instruments. Something

of the magnitude of these difficulties has been indicated in the literature [4,7,10].

When we speak of the solar constant we really are discussing a variable quantity, as it is generally recognized that solar emissions vary from time to time. However, for all practical purposes, the solar constant is the mean rate at which solar radiant energy (ultraviolet, luminous, and infrared) is present (per unit area) in free space at mean solar distance. Expressed mathematically, it is the total solar radiant energy received in gram-calories per square centimeter (langleys) per minute at the earth's mean distance from the sun. The accurate measurement of this constant, as well as the evaluation of any variations [3] that may occur in its value, has great significance in many fields.

The sun is a gaseous mass having a mean surface temperature of approximately 6,000° K. To the unaided eye it appears as a smooth circular disk. Magnified, the surface appears highly granulated and surrounded by a gaseous envelope, which, when examined under suitable conditions, is found to undergo much turmoil. In any case, this outer gaseous envelope produces the Fraunhofer absorption spectrum, which modifies markedly the visible and ultraviolet spectra of the solar emission. As a result, the effective radiating layer of the sun varies with wavelength (frequency of emitted radiation). That is, the effective solar temperature may be considerably below 6,000° K in the ultraviolet, whereas it may be significantly different in the infrared. A value near 7,000° K has been estimated for the far infrared at about 24 μ [12,13]. Hence sunspots, flares, or other disturbances in the solar surface may be expected to affect significantly not only the relative spectral emission from the sun, but also the total emission—the value of the solar constant.

No mention has been made of the radio emissions from the sun. Although such exist and indicate an effective solar temperature of around 1,000,000° K [14, 15], the energies involved are insignificant when compared with the normal blackbody radiation in the heat spectrum

[2] Figures in brackets indicate the literature references at the end of this paper.

[3] Measurements in the visible spectrum by Hardy and Giclas over a 5-year period indicated variations not exceeding 1.0 percent [11].

2. Instruments and Method

The instrumental setup (see fig. 1) employed in this work has resulted from experiences gained in connection with the measurement of the spectral distribution of the radiant energy from the sun at Washington and elsewhere during the past 5 years [16, 17, 18]. It consists primarily of a Carl Leiss double quartz-prism spectrometer mounted on a polar axis driven by a synchronous motor to follow (approximately) the path of the sun across the sky.

The use of this spectroradiometer mounted directly on a polar axis eliminates corrections previously required because of polarization effects introduced by reflections at variable angles from the heliostat mirrors and the faces of the optical components of the spectrometer. Also, optical errors introduced by improper adjustment of the heliostat or by solar declination change are no longer present. The spectrometer is simply aimed directly at the sun, which it then follows closely for hours without significant readjustment. Any departure due to changes in solar declination or to atmospheric refraction effects are detected by a photoelectric detector (also a visual indicator in the form of a directed light spot) and are corrected manually.

This spectroradiometer employs two 30-deg quartz prisms, through each of which the radiant energy makes a double pass. The collimating mirrors are spherical and coated with aluminum. The three slits are manually adjustable. The first and second slits were set for a mechanical opening of about 0.15 mm, and the third slit at 0.50 mm, for most of the data reported in the present case. With this instrument, changes in wavelength are accomplished by prism rotation, with a synchronous-motor drive attached to the wavelength drum. This unit permits recording at any one of three speeds, forward or reverse. A built-in clutch allows quick resetting of the wavelength drum, so that any part of the spectrum can be repeated at will.

The light beam was modulated at 510 cps by means of a sector disk mounted on a synchronous motor, and the output of the phototube was fed into a tuned amplifier. A strip recorder was used to register automatically the spectral data. A 935, emission-type phototube was employed as the detector in the ultraviolet and visible spectra to about 550 mμ. An Eastman lead sulfide photo-conducting cell was employed at longer wavelengths, extending to about 2.6 μ, where water vapor rendered the terrestrial atmosphere opaque to solar radiation.

All principal components of the setup are commercially available, except the tuned amplifier. This was built especially with an 11-step sensitivity-control (really a 33-step control because each of the three controls is separately adjustable) so as to cover a wide range of solar intensities. Fundamentally, the circuit layout is the same as that of an instrument previously described [19]. Experience has suggested several modifications, however, that have adapted its use more closely to the present work. Chief among these are the incorporation of the special 11-step sensitivity controls, the addition
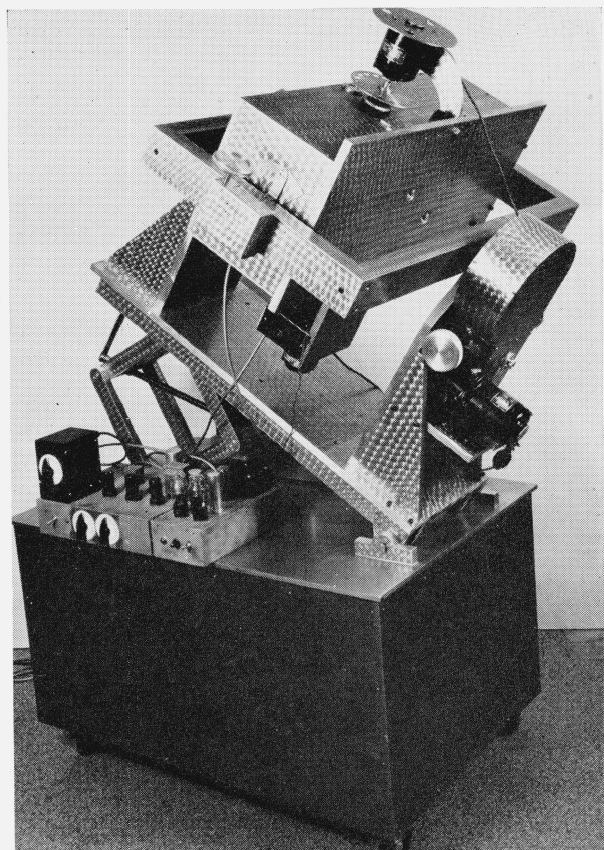

FIGURE 1. *Photograph of the spectroradiometer mounted on a polar axis.*

of a switch to adapt the amplifier for use with lead sulfide cells, a change in grid-bias voltage of the second amplifier stage to increase linearity in response, and additional filtering in the power supply to improve plate-voltage regulation. The revised circuit diagram is given in figure 2.

The instrument was set up outdoors, with the axis in a north-south direction as determined by the position of the sun at solar noon. Leveling screws at each corner of the instrument base (not shown in the photograph) made possible the precise placing of the instrument in a horizontal position. The instrument base thus furnished a level surface on which solar air-mass determinations could be made easily in terms of the shadow lengths of a cylindrical bar [20].

The operation of an instrument of this type on a polar axis is unusual but not entirely new [21]. The construction of this double monochromator lends itself to relatively satisfactory mounting in this manner, with only minor instrumental revisions, principally of increasing the spring tension holding the prisms in place. Slight flexing of the larger mirror mounts may be reduced by added adjustable bracing. The larger opening of the third slit eliminated most of the wavelength drift resulting from instrumental distortion as the spectroradiometer was rotated in following the sun.
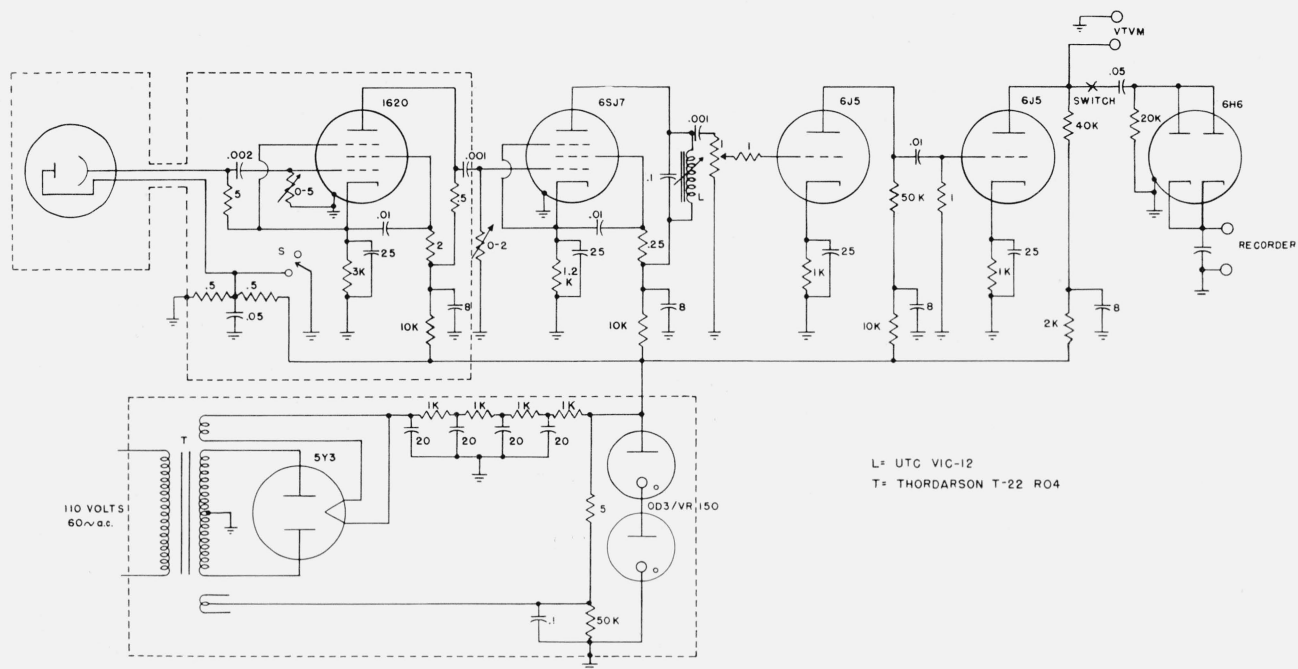
FIGURE 2. *Electronic circuit employed in 510-cycle-per-second tuned amplifier.*

Resistances in megohms and capacitances in microfarads except as otherwise noted.

Effects of instrumental temperature change were closely controlled through 24-hour operation of heating coils and a thermostat for keeping the spectrometer at a temperature near the highest point that would normally be approached in midafternoon. A housing of heavy aluminum, insulated inside with asbestos and outside with cork (not shown in the illustration), simplified temperature-variation problems. An auxiliary unit controlled the temperature of the PbS cell. No refrigeration was employed.

The wavelength scale was calibrated with a mercury-vapor lamp for the ultraviolet and visible spectra [19]. Water vapor, oxygen, and carbon-dioxide atmospheric absorption bands were employed in the infrared. The solar Fraunhofer bands furnished secondary wavelength standards and became the working wavelength references not only in recording but in the evaluation of the data.

A special tungsten-ribbon-filament-in-quartz lamp was employed in the spectral radiant-energy calibration of the entire spectroradiometer, including all the optical and electronic parts, as well as the recorder. This new lamp was more intense and more compact but otherwise similar to the standard lamps previously employed [17, 19]. The greater compactness of the lamp, together with the elimination of the heliostat, permitted the placing of the standard much closer to the entrance slit of the spectrometer, so that the calibrating intensities were increased by a factor of 10 or more above that previously possible.

Furthermore, for the spectral region of wavelengths between 296.7 and 435.8 mμ, a mercury-arc lamp was employed as a supplementary standard of radiant intensity. The relative intensities of the mercury lines from this source are known in this spectral region from laboratory measurements. The response of the spectroradiometer was calibrated from these mercury lines by normalizing their intensities against the tungsten continuum at 404.5 and 435.8 mμ.

The spectral distribution of the radiant energy of the tungsten-ribbon-filament-in-quartz lamp was established in terms of its color temperature (measured by the Colorimetry Section of the Bureau), the spectral emissivity of tungsten [4] as determined by DeVos [22], and the absolute radiant-energy output for selected wavelengths in terms of an NBS standard of thermal radiation [23, 24]. The first step of this evaluation involved the determination of the true temperature of the tungsten filament in terms of the color temperature ($2,854°K$, $C_2 = 14,380$) and the spectral emissivity of tungsten. A value of $2,790°K$ resulted from this calculation. Next, by employing blackbody data for this temperature and the spectral emissivities of tungsten (taken from the DeVos data), a relative spectral-energy curve for the tungsten-ribbon-filament was calculated. Finally, through the use of color filters the absolute radiant energy for the tungsten lamp was determined radiometrically for a number of selected spectral regions within the vicinity of some of the stronger mercury emission lines, which served as secondary radiant-intensity standards in carrying over the calibration from the thermal carbon-filament standards.

[4] It is realized that the published values of tungsten emissivity may not be precisely employed in the standardization of the particular tungsten-ribbon lamp used in this work. However, variations between different available lamps are small.

207

3. Spectral Solar-Energy Distribution

Most of the details relating to the reduction of the spectral distribution of the solar radiant energy (see table 1 and fig. 3) are omitted from this report. However, the methods were similar to those described in previous reports [16,17,18], for the ultraviolet and part of the visible portions of the spectrum.[5]

TABLE 1. *Spectral distribution of radiant energy from the sun for selected air masses, Sunspot, N. Mex.*

Altitude 9,200 feet. Mean for 4 days in June 1955. Radiant energy in microwatts per square centimeter per 10 $m\mu$ (corrected for mean solar distance). The M_0 factor in column 7 is the reciprocal of the atmospheric transmittance. The data in column 6, at wavelengths for which there are no entries in columns 2 to 5, are interpolations.

1	2	3	4	5	6	7	8
Wave-length	June 3 Air mass 1.00	June 4 Air mass 1.00	June 6 Air mass 1.00	June 7 Air mass 1.00	Mean Air mass 1.00	M_0 factor	I_0 Air mass 0
$m\mu$							
299.5					5.3	45	241
300.7					11.1	34	377
302.5	16.3			16.7	16.5	18.5	306
304	40.0	36.5	42.9	43.2	40.6	11.6	472
305.5					64.3	9.00	579
306	60.0	56.2	62.7	65.6	61.1	8.20	501
309.2					112	5.39	602
310	101	98	108	105	103	4.97	514
311.3					194	4.40	852
312	180	177	190	183	182	4.13	752
314					233	3.62	843
314.9					225	3.43	772
315.8					245	3.22	789
316.5	209	213	214	208	211	3.11	658
317.9					319	2.88	920
318.5	275	272	284	274	276	2.78	769
319.8					303	2.60	788
321.1					374	2.46	921
321.7					342	2.40	821
322.8					351	2.31	811
323.5	320	320	328	321	322	2.25	725
325.5					404	2.15	867
327.5					548	2.08	1,141
328.5	524	520	526	517	522	2.06	1,075
330.3					640	2.00	1,278
331.5	588	584	579	572	581	1.96	1,139
332.9					585	1.93	1,129
333.6					573	1.91	1,094
335.3					612	1.88	1,151
337	544	543	543	534	541	1.85	1,001
340.8					686	1.78	1,220
341.7					653	1.77	1,156
343.5					696	1.745	1,214
344.1	587	586	585	577	584	1.73	1,010
348.5					666	1.69	1,125
351.5					760	1.66	1,261
352.6					710	1.65	1,171
355.1					845	1.625	1,373
358.1	597	600	608	590	599	1.60	958
360					801	1.585	1,269
360.9	739	696	751	734	730	1.575	1,150
363.6					814	1.555	1,265
366.4					987	1.53	1,509
367.8					928	1.52	1,411
370					974	1.51	1,471
373.5	769	774	778	758	770	1.48	1,139
378.2					1,085	1.46	1,583
380					968	1.45	1,403
382.3					966	1.44	1,392
384					653	1.43	932

[5] Briefly, the effect of atmospheric attenuation on solar radiation was removed by assuming the validity of Beer's law and assuming that the thickness of the atmosphere is proportional to the secant of the zenith angle, x. The "Optical Air Mass" is defined as $\sec x$, and the data for various angles x are plotted as $\log I$ versus $\sec x$, and the resulting straight lines are extrapolated to $x=0$, or zero air mass.

TABLE 1. *Spectral distribution of radiant energy from the sun for selected air masses, Sunspot, N. Mex.*—Continued

1	2	3	4	5	6	7	8
Wave-length	June 3 Air mass 1.00	June 4 Air mass 1.00	June 6 Air mass 1.00	June 7 Air mass 1.00	Mean Air mass 1.00	M_0 factor	I_0 Air mass 0
$m\mu$							
387					846	1.42	1,202
391					1,086	1.40	1,521
393.4	683	689	688	680	685	1.39	952
396					955	1.375	1,314
396.9					805	1.37	1,103
403.5					1,514	1.34	2,029
406.4	1,414	1,434	1,424	1,395	1,417	1.33	1,884
410.2					1,426	1.31	1,868
416.7					1,495	1.295	1,937
420.7					1,500	1.28	1,920
423.5					1,429	1.27	1,815
427.2	1,182	1,201	1,196	1,177	1,189	1.26	1,498
432.5					1,361	1.25	1,701
438.3	1,454	1,454	1,448	1,431	1,447	1.24	1,794
440.5					1,610	1.23	1,980
450.8	1,732	1,743	1,732	1,711	1,730	1.22	2,110
455.6					1,732	1.205	2,087
465	1,725	1,740	1,709	1,694	1,717	1.19	2,043
482					1,843	1.18	2,175
487	1,702	1,711	1,694	1,675	1,695	1.175	1,992
497					1,871	1.17	2,188
500	1,851	1,856	1,843	1,813	1,841	1.17	2,154
509					1,900	1.16	2,204
518	1,778	1,781	1,778	1,742	1,770	1.155	2,044
527					1,892	1.15	2,175
530	1,932	1,959	1,950	1,913	1,938	1.15	2,229
535					1,865	1.15	2,145

For the spectral region from about 540 $m\mu$ to 2.5 μ covered by the lead sulfide-cell measurements a slightly different technique was required in the determination of the spectral radiant-energy emission of the sun. Although the lead sulfide cell was enclosed in a sealed brass box (constructed of massive material of thicknesses ranging from $\frac{1}{4}$ to $\frac{3}{8}$ in.) and thermostatically controlled so that temperature and humidity conditions were relatively constant, large changes in sensitivity occurred from time to time, so that direct standard-lamp calibrations (although made several times each day) could not be relied upon. Hence, measurements at two wavelengths in the visible spectrum (428 and 487 $m\mu$), which were repeatedly scanned every few minutes along with the infrared spectrum, were employed in establishing the energy levels throughout the infrared spectrum. In doing this it was assumed that the solar intensity at these key wavelengths remained the same during the time the work was in progress (June 3 to 19). This assumption is probably true within the limits of the experimental data [11]. Reference to table 1 indicates the small spread found in the observed intensity at these wavelengths for the 4 days upon which the infrared data are based.

Furthermore, within the infrared spectrum a number of intense water-vapor bands exist. The principal ones near 942, 1,135, 1,379, and 1,872 $m\mu$ extend over relatively wide spectral regions and have intense absorption, so that the usual variations occurring in the concentration of water vapor in the atmosphere above the Sacramento Mountains prohibited the use of any wavelengths within the immediate vicinity of these regions in the evaluation
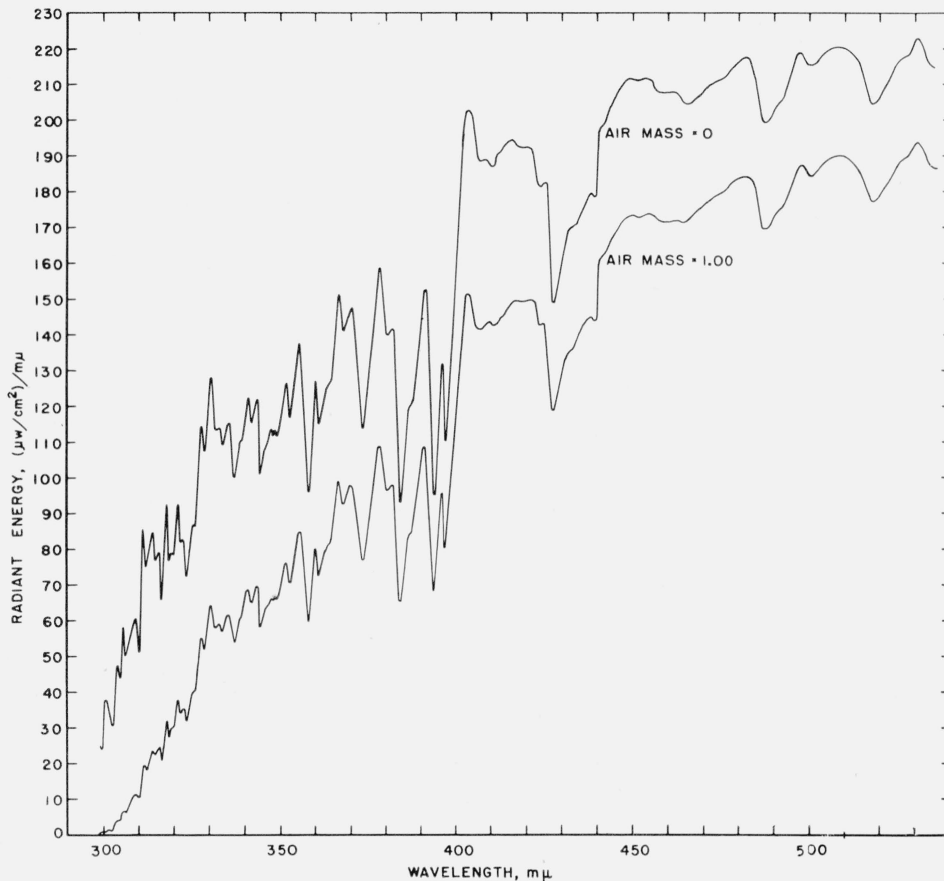
FIGURE 3. *Spectral distribution of the radiant energy from the sun.*

Sunspot, N. Mex., June 1955. (Mean of 4 days.)

of the data. Hence, it was necessary to choose a group of wavelengths that was little affected by water vapor in the extrapolations and calculations of the spectral solar radiant energy in the infrared region between the visible and 2.5 μ. Although the 4 days (June 16, 17, 18, and 19) for which the data were reduced were exceptionally dry for the location, the water-vapor absorption was very intense and therefore very sensitive to small changes in the total water content of the atmosphere. This high sensitivity to small changes in atmospheric water content has been recognized in the development of absolute humidity meters [25].

4. Atmospheric Transmittance and Ozone

The atmospheric transmission curve calculated on the basis of the data for the 4 days (June 3, 4, 6, and 7) is given in figure 4. In this illustration the logarithm of the observed transmittances of unit atmosphere has been plotted against a function of the wavelength. In order to obtain a straight line within those spectral regions in which there is no atmospheric absorption, the wavelength scale has been expanded according to the function $-(\mu-1)^2 \lambda^{-4}$ of Rayleigh's law of molecular scattering [26].
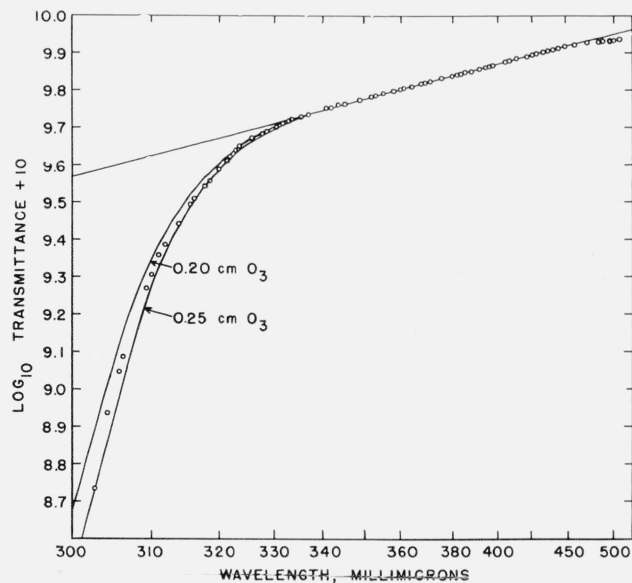

FIGURE 4. *Atmospheric transmittance at Sunspot, N. Mex., altitude 9,200 feet; also determination of total ozone above the observing station.*

Upper curve, scattering; lower curves, ozone; circles, atmospheric transmittance; air mass, 1.00; wave length scale as a function of $-(\mu-1)^2\lambda^{-4}$.

209

The selective absorption at wavelengths shorter than about 340 mμ is assumed to result from ozone. The amount of absorption is hence a measure of the total ozone concentration in the upper atmosphere.

In order to translate the specific absorption data in the wavelength region below 340 mμ into precise amounts of ozone, the absorption coefficients for the pure gas reported by Fabry and Buisson have been employed [27] in the calculations of the two curves (fig. 4) representing the amounts of ozone required for a similar amount of optical absorption. On the basis of these data, about 0.22 to 0.23 cm of ozone (ntp) was present at the time this investigation was in progress. This is in close agreement with previous measurements at this station for this season of the year [18, 28].

5. Evaluation of the Solar Constant

The spectral range covered in this work includes most of the solar radiant energy reaching the earth's surface. Its use in an integration of the solar emission, calculated for outside the terrestrial atmosphere for mean solar distance (per unit area), results in a radiant-energy value known as the solar constant, Q, when defined in terms of gram-calories per square centimeter (langleys) per minute.

The evaluation of Q requires three steps; first an integration of the data recorded herein (see fig. 3) for air mass 0, that is, outside the atmosphere within the limits of observation—300 to 2,500 mμ; second, a correction for mean solar distance; and third, corrections for unmeasured ultraviolet and infrared radiant energy of wavelengths shorter than 300 mμ and longer than 2,500 mμ.

The integrated values resulting as the mean for 4 days wherein measurements were made through the spectral region of 300 to 540 mμ and for the 4 days wherein measurements were made through the spectral region of about 320 to 2,600 mμ are given in table 2. These values have been increased already by 2.94 percent, the amount to correct them for mean solar distance. The correction in the ultraviolet for wavelengths below 300 has been made by arbitrarily extrapolating the solar energy curve to zero within the spectral region of about 200 to 220 mμ.[6] The infrared correction of 0.06 gram-calories per square centimeter per minute has been added as the probable value of solar radiant energy for wavelengths longer than 2.5 μ [5] based on a blackbody curve at the solar temperature. This results in a value of 2.05 gram-calories per square centimeter per minute as a preliminary measured value of the solar constant, Q, by this method. This value is probably correct to less than 5 percent and is in general agreement with recent estimates [4, 5, 18], being a little higher than those usually reported by the Smithsonian Institution.

TABLE 2. *Integrated spectral distribution of solar radiant energy for air mass 0*

Center of wavelength interval	Radiant energy	Center of wavelength interval	Radiant energy	Center of wavelength interval	Radiant energy
mμ	$\mu w/cm^2$	mμ	$\mu w/cm^2$	mμ	$\mu w/cm^2$
300	1,857	497.5	1,089	865	1,005
302.5	200	502.5	1,084	875	985
307.5	279	507.5	1,100	885	968
312.5	378	512.5	1,096	895	948
317.5	388	517.5	1,043	905	930
322.5	410	522.5	1,050	915	911
327.5	521	527.5	1,097	925	894
332.5	578	535	2,113	935	876
337.5	548	545	2,138	945	859
342.5	586	555	2,113	955	842
347.5	551	565	2,086	965	826
352.5	621	575	2,053	975	809
357.5	585	585	2,018	985	793
362.5	613	595	1,982	995	778
367.5	624	605	1,994	1,005	762
372.5	665	615	1,906	1,015	746
377.5	691	625	1,868	1,025	732
382.5	666	635	1,829	1,035	718
387.5	592	645	1,790	1,045	703
392.5	623	655	1,754	1,055	689
397.5	696	665	1,707	1,065	675
402.5	1,009	675	1,662	1,075	661
407.5	940	685	1,614	1,085	646
412.5	947	695	1,564	1,095	632
417.5	972	705	1,513	1,150	5,707
422.5	929	715	1,463	1,250	4,715
427.5	818	725	1,415	1,350	3,916
432.5	869	735	1,367	1,450	3,194
437.5	923	745	1,321	1,550	2,541
442.5	1,021	755	1,278	1,650	1,951
447.5	1,058	765	1,242	1,750	1,446
452.5	1,054	775	1,213	1,850	1,102
457.5	1,049	785	1,187	1,950	947
462.5	1,050	795	1,164	2,050	830
467.5	1,027	805	1,139	2,150	711
472.5	1,035	815	1,115	2,250	653
477.5	1,061	825	1,093	2,350	593
482.5	1,072	835	1,069	2,450	558
487.5	1,000	845	1,047		
492.5	1,055	855	1,025		

Total $\mu w/cm^2$ for wavelengths shorter than 2,500 mμ=139,164
Total gram-calories cm^{-2}/min for wavelengths shorter than 2,500 mμ=1.99
Correction for wavelengths longer than 2,500 mμ=0.06
Total value of solar constant, Q=2.05

6. Discussion of the Data

This work is a continuation of that previously initiated and has offered an opportunity to test the merits of certain changes in the original equipment [16, 17, 18]. Although on many days clouds or dust interfered with the work, there were 8 days (4 when the ultraviolet phototube was set up and 4 when the lead sulfide cell was employed) on which little interference resulted from dust or clouds. Only the data obtained on these days have been used in the reductions for the spectral-energy distributions and for the integration of the value of the solar constant, Q. This work involves radiant-energy evaluations of a highly complicated nature, so that there are numerous points at which errors or uncertainties may enter. Hence, the accuracy cannot be claimed to be better than plus or minus a few percent. However, the preliminary evaluation of the solar constant by this method indicates something of the possibilities that exist in this field. Improvements of the equipment

no doubt account for certain variations between the data recorded herein and those previously reported at Climax [17] and at Sacramento Peak [18]. Others possibly result from solar changes within the interval. Future measurements of a still higher accuracy should furnish much valuable information on the character of the solar radiation and the magnitude of its variations.

The spectral-energy values, as well as the integrated total (solar Q) intensities, are dependent very much upon the adopted values for the spectral emissivity of tungsten. Hence, if it is later found that erroneous values for the spectral emissivity of tungsten have been employed in this work, a correction to the data recorded herein will be required. Basic to the comparison of Smithsonian value of the solar constant and that here derived is the comparison of the radiometric standards used by the Bureau and the Smithsonian Scale of Pyrheliometry.

7. References

[1] E. O. Hulburt, The upper atmosphere of the earth, J. Opt. Soc. Am. **37**, 405 (1947).

[2] J. L. Greenstein, H. E. Clearman, and E. Durand, Upper atmosphere studied from rockets, G. P. Kuiper, ed., The atmospheres of the earth and planets (Univ. of Chicago Press, Chicago, Ill., 1949).

[3] L. B. Aldrich and W. H. Hoover, The solar constant, Science **116,** 3 (Dec. 12, 1952).

[4] Francis S. Johnson, The solar constant, J. Meteorol. **11,** No. 6, 431 (1954).

[5] M. Nicolet, Sur le probléme de la constante solaire, Ann. astrophys. **14,** 249 (1951).

[6] C. G. Abbot, A revised analysis of solar-constant values, Smithsonian Inst. Misc. Publs. No. 3902 (1947).

[7] Evry Schatzman, Sur la valeur de la constante solaire, Ann. astrophys. **12,** 305 (1949).

[8] C. G. Abbot and L. B. Aldrich, Ann. Astrophysical Observatory of the Smithsonian Inst. **3,** 21, 73 (1913).

[9] C. G. Abbot, Ann. Astrophysical Observatory of the Smithsonian Inst. **4,** 99 (1922).

[10] M. Minnaert, The photosphere, G. P. Kuiper, ed., The Sun (Univ. Chicago Press, Chicago, Ill., 1953).

[11] R. H. Hardie and H. L. Giclas, A search for solar variation, Astrophys. J. **122,** 460 (1955).

[12] A. Adel, Selected topics in infrared spectroscopy of the solar system, G. P. Kuiper, ed., The atmospheres of the earth and planets (Univ. Chicago Press, Chicago, Ill., 1949).

[13] R. Peyturaux, Contribution a l'étude du fond continu du spectre solaire dans le Proche infra-rouge, Ann. Astrophys. **15,** 302 (1952).

[14] S. K. Mitra, The upper atmosphere (The Asiatic Society, Calcutta, 1948).

[15] A. V. Haeff, On the origin of solar radio noise, Phys. Rev. **75,** 1546 (1949).

[16] Ralph Stair, Ultraviolet spectral distribution of radiant energy from the sun, J. Research NBS **46,** 353 (1951) RP2206.

[17] Ralph Stair, Ultraviolet radiant energy from the sun observed at 11,190 feet, J. Research NBS **49,** 227 (1952) RP2357.

[18] Ralph Stair, Russell G. Johnston, and Thomas C. Bagg, Spectral distribution of energy from the sun, J. Research NBS **53,** 113 (1954) RP2523.

[19] Ralph Stair, Photoelectric spectroradiometry and its application to the measurement of fluorescent lamps, J. Research NBS **46,** 437 (1951) RP2212.

[20] Ralph Stair, The spectral radiant energy from the sun through varying degrees of smog at Los Angeles (Proceedings of the third Air Pollution Symposium, Pasadena, California, April 1955).

[21] W. W. Coblentz and H. Kahler, A new spectropyrheliometer and measurements of the component radiations from the sun and from a quartz mercury vapor lamp, BS Sci. Papers **16,** 233 (1920) S378.

[22] J. C. DeVos, The emissivity of tungsten ribbon. The tungsten striplamp as a standard source of radiation (Thesis, Univ. Amsterdam, 1953); see also, Physica **20,** 690 and 715 (1954).

[23] W. W. Coblentz, Measurements on standards of radiation in absolute value, Bul. BS **11,** 87 (1915) S227.

[24] Ralph Stair and Russell G. Johnston, Effects of recent knowledge of atomic constants and of humidity on the calibrations of the National Bureau of Standards thermal-radiation standards, J. Research NBS **53,** 211 (1954) RP2535.

[25] L. W. Foskett, N. B. Foster, W. R. Thickstun, and R. C. Wood, Infrared absorption hygrometer, Monthly Weather Rev. **81,** 267 (1953).

[26] Edison Pettit, Spectral energy-curve of the sun in the ultraviolet, Astrophys. J. **91,** 159 (1940).

[27] C. Fabry and H. Buisson, Data on ozone absorption, Compt. rend. **192,** 457 (1931).

[28] Ralph Stair, Filter radiometry and some of its applications, J. Opt. Soc. Am. **43,** 971 (1953).

WASHINGTON, April 20, 1956.